New high resolution headmodel for accurate electromagnetic field computation

L. M. Angelone[1,2], S. Tulloch[3], G. Wiggins[1], S. Iwaki[1], N. Makris[3], G. Bonmassar[1]

[1]Athinoula A. Martinos Center for Biomedical Imaging, Massachusetts General Hospital, Charlestown, MA, United States, [2]Biomedical Engineering Department, Tufts University, Medford, MA, United States, [3]Center for Morphometric Analysis, Massachusetts General Hospital, Charlestown, MA, United States

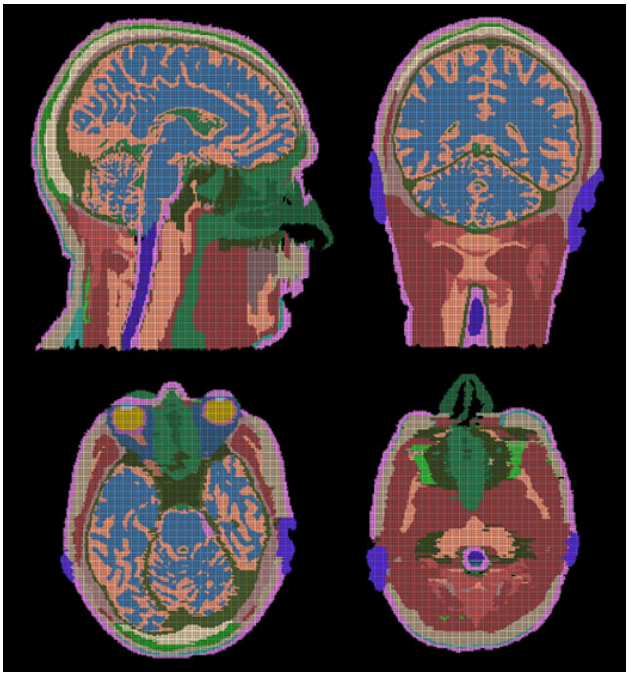

Figure 1. *High-resolution head model from realistic MRI data. Twentynine tissues were segmented. (Top-left) Sagittal view. (Top-right) Coronal view. (Bottom left and right) Axial View.*

INTRODUCTION. Realistic head models are commonly used for the computation of the electromagnetic fields, which are mostly used for RF coil design and safety studies [1-4]. The resolution of the head model generally affects the accuracy of the electromagnetic field computation.

METHODS. One high-resolution head model ($1\times1\times1mm^3$) was manually segmented from the anatomical MRI data of an adult male subject. The subject anatomical MRI was performed with a quadrature birdcage transmit/receive head coil on our 1.5T scanner (General Electric, Milwaukee, WI, USA). Three whole-head scans were collected with a T1-weighted 3D-SPGR sequence (TR/TE=24/8ms) with 124 slices, 1.3mm thick (matrix size 256×192, FOV 256mm). The individual images were motion-corrected and averaged to increase gray/white matter contrast-to-noise ratio using MEDx software (Sensor Systems, Inc., Sterling, VA, USA). Twenty six different types of tissue were manually segmented from the MRI images: Adipose, Air, Bone, Aqueous Humor, Connective Tissue, Cornea, CSF_SA, Diploe, Dura, Ear, Epidermis, Inner Table, Lens, Muscle, Nasal Structures, Nerve, Orbital-Fat, Outer-Table, Subcutaneous Tissue, Retina/Cornea/Sclera, SC-Fat/Muscle, Soft-Tissue, Spinal Cord, Teeth, Tongue, Vitreous-Humour. The brain was separately segmented using a hybrid method combining watershed algorithms and deformable surface techniques [5]. Using a three-component mixture model, whose parameters were computed during the skull-stripping process, the brain was segmented into cerebrospinal fluid (CSF), gray matter and white matter. The segmentation of the brain was then imported and coregistered to the high-resolution head model using MATLAB (Mathworks Co., Natick, MA, USA). A total of 29 tissues were obtained for the head model (**Fig. 1**). The dimensions of the head model were 171mm from left to right, 218mm from back to front, and 240mm high.

The head model was used for evaluation of RF power distribution in MRI using FDTD algorithm (XFDTD, REMCOM Co., State College, USA). Each cell of the head model was isotropic and of dimensions $1\times1\times1mm^3$. The physical properties of tissue were selected according to the literature [6]. The total number of Yee cells [7] for the head models was 4642730. The total volume considered including the free space around the model was $296\times390\times351mm^3$. Simulation studies with the head model were conducted with birdcage coil [4] at 128MHz-3T and 300MHz-7T.

RESULTS AND DISCUSSION. The simulated B-field showed the typical dielectric resonance at 7T [8]. The B-field distribution was in general much closer to the real case (**Fig. 2 left**) since it showed positive peaks in the ventricles (**Fig. 2 center**) whereas the 8-tissues head model with the same resolution (**Fig. 2 right**) showed a negative peak in the midbrain region. The peak of SAR was in the Nasal structures, near a source [3]. Local SAR increases could be partly enhanced due to staircasing effects [9]. However the high number of cells per wavelength (2000 cells at 128 MHz, 1000 cells at 300 MHz) should reduce the staircase error to less than 1dB [10]. Furthermore, the position of the peak SAR values were consistent with the literature [3, 11].

CONCLUSIONS. We present a new high resolution head model that can be a usefully utilized for electromagnetic fields computation. Results obtained are in agreement with the literature and outperform the accuracy in estimating the distribution of the B_1 field of a model with same resolution but with a lower number of tissues.

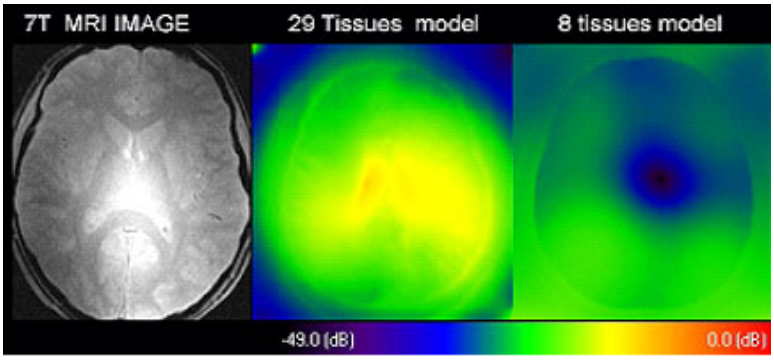

FIGURE 2 *(left) MRI image showing the typical dielectric resonance at 7T localized in the center. (Middle) B1 field distribution calculated with the new head model (center) compared with 8 tissues head model (right) using birdcage coil at 7T.*

ACKNOWLEDGEMENT. We thank David Carpenter of REMCOM, George Papadimitriou, Andreas Potthast, Chris Wiggins, Larry Wald and Bruce Rosen. This work was supported by NIH grant R01 EB002459-01 and P41 RR014075.

REFERENCES. 1. Collins, C.M., et al., Magn Reson Med, 1998. 40(6): p. 847-56. **2.** Jin, J., et al., Magn Reson Med, 1997. 38(6): p. 953-63. **3.** Ibrahim, T.S., et al., Phys Med Biol, 2001. 46(2): p. 609-19. **4.** Angelone, L.M., et al., Bioelectromagnetics, 2004. **25**(4): p. 285-95. **5.** Dale, A.M., et al., Neuroimage, 1999. 9(2): p. 179-94. **6.** FCC, http://www.fcc.gov/fcc-bin/dielec.sh **7.** Yee, K.S., IEEE Transactions on Antennas and Propagation, 1966. 14(3): p. 302-307. **8.** Vaughan, J.T., et al., Magn Reson Med, 2001. 46: p. 24-30. **9.** Cangellaris, A.C., et al., IEEE Transactions on Antennas and Propagation, 1991. 39: p. 1518-1525. **10.** Holland, R., IEEE Trans on Electromagnetics Compatibility, 1993. 35(4): p. 434-38. **11.** Chou, C.K., et al., Bioelectromagnetics, 1996. 17(3): p. 195-208.